Biochimica et Biophysica Acta, 1108 (1992) 40–48

BBAMEM 75680

Repulsive interactions and mechanical stability of polymer-grafted lipid membranes

D. Needham [a], T.J. McIntosh [b] and D.D. Lasic [c]

[a] *Mechanical Engineering and Materials Science, Duke University, Durham, NC (USA).* [b] *Department of Cell Biology, Duke University Medical Center, Durham, NC (USA) and* [c] *Liposome Technology Inc. Menlo Park, CA (USA)*

(Received 26 March 1992)

Key words: Stealth liposome; Polymer grafting; Lipid bilayer; Poly(ethylene glycol); X-ray diffraction; Steric stabilization; Membrane mechanical properties

Liposome membranes containing lipids with covalently attached poly(ethylene glycol) (PEG-lipid) are currently being developed as drug delivery systems. These, so called, 'Stealth®' liposomes have a relatively long half life (~ 1 day) in blood circulation and show an altered biodistribution *in vivo*. The extended lifetime appears to result from a steric stabilization of the liposome by the grafted polymer. In order to characterize the surface structures that promote steric stability in such polymer-grafted lipid bilayer systems, we have used X-ray diffraction to measure the structural organization and interbilayer repulsion for lipid/cholesterol (2:1) bilayers incorporating 4 mol% of a PEG-lipid in which the molecular weight of the PEG moiety was 1900 g/mol. At this concentration, applied pressure versus interbilayer distance relations showed that the grafted polymer moiety extended ~ 50 Å from the lipid surface and gave rise to a strong, slowly decaying repulsive pressure between membranes that opposed their close approach. Also, the pressure vs. distance relations were only modestly altered by changing the ionic strength of the medium (1 mM NaCl and 100 mM NaCl). Therefore, even though the PEG-lipid headgroup bears a negative charge, the long range pressure cannot be due primarily to an electrostatic double layer pressure. Measurements of lipid bilayer elasticity using micropipet manipulation showed that PEG-lipid did not change the cohesive properties of lipid/cholesterol liposomes which was consistent with the X-ray structural data showing that the PEG-lipid did not change the normal structure of the bilayer interior. From these data we conclude that the repulsive barrier properties of lipid-grafted PEG polymer chains originate mainly from a steric pressure and that this simple polymer steric stabilization is the basis for the extended *in vivo* circulation times observed for polymer-grafted liposomes.

Introduction

The presence of certain adsorbed or grafted polymers at the interface between biofluids and biomaterials is currently attracting considerable attention because of the repulsive properties that these polymers possess. For example, a newly developed strategy based on lipid-grafted-polymer is leading to the availability of a more effective liposome drug delivery system. Like other colloidal particles [1], drugs and conventional liposomes [2] are usually rapidly cleared from the circulation by the reticuloendothelial system (RES). However, the uptake of liposomes by the RES can be significantly inhibited by incorporating bilayer-compatible species such as poly(ethylene glycol)-linked lipids (PEG-lipid) or the ganglioside G_{M1} [3–12]. This strategy results in an increase in liposome circulation time and leads to an altered biodistribution of the polymer-bearing liposomes. The term 'Stealth' liposome [13] was coined to describe this evasive property and the PEG-lipids in particular are commonly referred to as Stealth® lipids [14]. Interest in surface polymers also extends to other developments concerning solid biomaterials, where the attachment of similar polymers is being investigated in order to minimize or prevent the adsorption of proteins and cells from the bloodstream [15–19] and as model polymer covered surfaces [20].

Several workers have recently measured a range of extended liposome circulation times [5–12] and liposome aggregation *in vitro* [21] for different lipid compositions containing 2–10 mol% PEG-lipids in which the molecular weight of the PEG moiety was between 750 g/mol and 5000 g/mol. Although such liposome formulations have shown reduced biofluid interactions and have prolonged encapsulated-drug circulation times to several days, mechanisms of recognition-evasion and liposome blood clearance are still not fully understood. It has been postulated that the mecha-

Correspondence to: D. Needham, Mechanical Engineering and Materials Science, Duke University, Durham, NC 27706, USA.

nisms at the root of the evasive property lie in a steric stabilization of the liposome surface by the grafted polymer [6,8–10,22]. Steric stabilization by the polymer is expected to oppose the mutual aggregation that has been found to occur between unmodified lipid surfaces [23–27] and would also appear to limit the interactions of liposomes with all other cellular surfaces in the blood system. In addition, the presence of surface polymer inhibits protein adsorption [9,18,19] and so may prevent destabilization and disintegration of liposomes by the action of plasma lipoproteins [28,29]. Recent experimental studies have in fact shown that the total protein binding to liposomes that have been briefly exposed to whole blood *in vivo* is inversely correlated with liposome clearance [30]. The PEG polymer should also inhibit opsonization by immunoglobulins that trigger specific uptake of the liposomes by macrophages [6,9,12,31]. In addition to these interfacial mechanisms, the cohesive properties of the lipid bilayer [32] are expected to be important factors in determining the physical and chemical stability and immuno-labelling of liposomes in the bloodstream.

Whilst polymers that are adsorbed or grafted onto a variety of solid substrates have been the subject of considerable theoretical and experimental investigation [20,33–35], to our knowledge there has been only one measurement of polymer chain extension away from an actual lipid bilayer surface and this was for a PEG surfactant (nonyl-phenyl PEG) [36]. Thus, the motivation for our present study was to begin to characterize the surface structures that appear to promote steric stability in polymer-grafted lipid bilayer sytems. Our initial studies aim to: (i) provide the first direct measurements of the extension of lipid-grafted poly(ethylene glycol) chains from the surface of a lipid bilayer, (ii) measure the mutual repulsive pressures that adjacent interacting polymer-lipid surfaces are expected to exert, (iii) determine whether Stealth liposomes themselves will come into adherent contact, and (iv) measure the effect of incorporating PEG-lipids on bilayer mechanical stability. The results of these kinds of experiments should help us to evaluate mechanisms of biosurface stabilization and liposome blood clearance and to test current grafted-polymer theories [20,33–35,37–39].

Materials and Methods

Materials

For both X-ray and micropipet experiments, lipids were chosen to be similar to typical formulations currently being tested *in vivo*. In these experiments the Stealth lipid consisted of a poly(ethylene glycol) (PEG) polymer (1900 g/mol, degree of polymerization of ~ 43 mers), that was covalently bonded to a lipid molecule (*N*-(carbamyl-poly(ethylene glycol methyl ether)-1,2-distearyl-*sn*-glycero-3-phosphoethanolamine, sodium salt, from Liposome Technology Inc., Menlo Park CA, commonly abbreviated to $DSPE^{1900}PEG$). Here, the polymer lipid is simply referred to as PEG-lipid. 4 mol% of this PEG-lipid was incorporated into lipid bilayers so that the PEG was essentially grafted at the surface of the bilayer and is thus distinct from adsorbed polymer systems. Stealth bilayers consisted of stearoyloleoylphosphatidylcholine (SOPC)/ cholesterol(C) at a mol ratio of 2 : 1 with the PEG-lipid included at 4 mol%. 'Conventional' lipid bilayers (without PEG-lipid) were composed of SOPC/C at mol ratios of 2 : 1.

SOPC was obtained from Avanti Polar Lipids. Cholesterol, poly(vinylpyrrolidone) (PVP) (average molecular weight of 40000), and dextran (average molecular weight of 255000) were obtained from Sigma Chemical Corp. PVP and dextran osmoticant solutions of 0 to 40% w/w were made in either 1 mM or 100 mM NaCl in triply distilled water.

X-ray diffraction

In order to directly quantify mutual repulsion between free-standing lipid surfaces containing grafted-polymer, we have used an X-ray diffraction method to study osmotically stressed multilamellar lipid preparations. This method has proven utility in measuring a range of interbilayer repulsive pressures such as short range steric, hydration, electrostatic, and fluctuation interactions [40–47]. Low- and wide-angle X-ray diffraction patterns were recorded from bilayers subjected to applied osmotic pressures, as both unoriented dispersions in polymer solutions and as oriented multilayers in relative humidity atmospheres.

For the unoriented multiwalled liposomes, osmotic pressure was applied by the method of LeNeveu et al. [40]. In brief, an excess amount of a solution of a neutral polymer, either PVP or dextran was added to the dry lipid. Because PVP and dextran molecules are too large to enter between the lipid multilayers, they compete for water and apply an osmotic pressure to the lipid multilayers [40,48]. Osmotic pressures for the PVP and dextran osmoticant solutions have been previously measured [48] and range from $1.1 \cdot 10^5$ to $3.2 \cdot 10^7$ dyne/cm^2. The validity of the assumption that the polymer did not enter the lipid lattice was demonstrated by experiments in which the dry lipid was separated from the polymer solution by a dialysis membrane. Similar diffraction patterns were recorded in osmotic stress experiments in the presence and absence of the dialysis bag. Moreover, the same diffraction patterns were recorded from specimens equilibrated in either PVP or dextran solutions of equivalent osmotic pressures. The lipid-osmoticant suspensions were covered with nitrogen and incubated for several hours with periodic vortexing above the lipid's main

phase transition temperature. Several freeze-thaw cycles were employed to assure that the NaCl solution was uniformly distributed throughout the multilayers. The lipid-polymer suspensions were sealed in quartz glass capillary tubes and mounted in a point-collimation X-ray diffraction camera [41–43,46].

Oriented multilamellar specimens were formed by placing a small drop of lipid-chloroform solution on a piece of aluminum foil and slowly evaporating the chloroform. The foil substrate was given a convex curvature and mounted in a controlled humidity chamber on a line-focussed single-mirror X-ray camera, where the X-ray beam was oriented at a grazing angle relative to the lipid multilayers. The humidity chamber consisted of a canister with two mylar windows for passage of the X-ray beam. Pressures in the range of $2.8 \cdot 10^7$ to $5.8 \cdot 10^8$ dyne/cm^2 were applied through the vapor phase to the oriented lipid multilayers by the use of established procedures [42,49]. The vapor pressure was controlled by means of a cup of saturated salt solution in the chamber. To speed equilibration, a gentle stream of nitrogen gas was passed through a flask of the saturated salt solution and through the chamber.

For all specimens (oriented multilayers and unoriented lipid-osmoticant suspensions), X-ray diffraction patterns were recorded at 20°C on Kodak DEF X-ray film. The films were densitometerd with a Joyce-Loebl microdensitometer as described previously [41,42]. After background subtraction, integrated intensities, $I(h)$, were obtained for each order h by measuring the area under each diffraction peak. For unoriented patterns, the structure amplitude $F(h)$ was set equal to $\{h^2 I(h)\}^{1/2}$ [50,51]. For the oriented line-focussed patterns the intensities were corrected by a single factor of h due to the cylindrical curvature of the multilayers [50,51] so that $F(h) = \{hI(h)\}^{1/2}$.

Electron density profiles, $\rho(x)$, on a relative electron density scale were calculated from

$$\rho(x) = (2/d)\sum \exp\{\phi(h)\} \cdot F(h) \cos(2\pi x h / d) \qquad (1)$$

where x is the distance from the center of the bilayer, d is the lamellar repeat period, $\phi(h)$ is the phase angle for order h, and the sum is over h. Phase angles were determined by the use of the sampling theorem [52] as described in detail previously [53]. All electron density profiles described in this paper are at a resolution of $d/2h_{max} \approx 6$ Å.

Micropipet manipulation

The mechanical stability of individual liposomes was determined by using a micropipet manipulation method that measured the elastic area expansion modulus K, and the tensile strength of the bilayers. The preparation of giant liposomes is well documented in several recent publications concerning the micromanipulation of such structures [32,54]. Briefly, lipid/cholesterol mixtures were made in a chloroform/methanol solution and liposomes were formed by gentle rehydration of dried lipid lamellae from a teflon substrate using sucrose solutions (160 mosM). The sucrose-containing liposome sample was diluted with 180 mosM glucose and added to the manipulation chamber on the video microscope stage. Although few in number, large unilamellar (20–40 μm diameter) liposomes were identified for the aspiration test. The slight deflation of the liposomes in the hyperosmotic media produced a small projection in the suction pipet. After a pre-stress, the pipet suction pressure was increased, decreased and finally increased again in increments to produce liposome lysis (failure). The corresponding change in liposome projection length in the pipet was recorded on video.

Subsequent analysis of pipet and liposome geometry allowed the calculation of the relative membrane area change α (liposome area change, ΔA, divided by an initial, low stress area A_0) in response to induced membrane tension τ due to liposome pressurization [54]. The changes in projection length in the pipet were solely due to changes in isotropic membrane tension and not volume changes. Membrane isotropic tension was then plotted versus membrane area change, for membrane tensions greater than ~ 0.5 dyne/cm [32].

In order to make a direct test of the expected non-adherence property of Stealth liposomes we used another micropipet manipulation technique employing two micropipets [25,27]. Two liposomes were transfered into 100 mM NaCl solution, maneouvered into close proximity but not forced into contact, and the pipets were then left in these fixed positions. In this experimental method, the extent of adhesive spreading of one liposome onto the other was controlled by pipet suction pressure. One liposome was held under high tension (~ 3 dyne/cm) so that it formed a rigid spherical test surface, whilst the other was held under lower, variable suction pressure. In this test, spontaneous adhesion is allowed to occur in discrete, equilibrium steps controlled by pipet suction pressure applied to the spreading liposome. The adhesion energy is then calculated from the pipet suction pressure and pipet and liposome geometries.

Results

Applied pressure versus lamellar repeat period

For each specimen of SOPC/C or SOPC/C with 4 mol% PEG-lipid, the X-ray diffraction pattern consisted of from 3 to 8 low-angle reflections, which indexed as orders of a lamellar repeat period, and a single wide-angle band centered at 4.5 Å. These patterns are typical of lipid bilayers in the liquid-crystalline phase [55]. For both SOPC/C and SOPC/C/

PEG-lipid bilayers, the position and width of the wide-angle pattern was independent of applied osmotic pressure.

We first consider X-ray experiments for liposomes in 100 mM NaCl and in relative humidity atmospheres. A plot of the data for SOPC/C bilayers with and without PEG-lipid is shown in Fig. 1 as logarithm of applied pressure versus lamellar repeat period. For 2:1 SOPC/C bilayers, the lamellar repeat period ranged from 67.0 Å for an applied pressure of $P = 1.6 \cdot 10^5$ dyne/cm^2 (liposomes in 4% PVP in 100 mM NaCl) to 55.8 Å at $P = 5.8 \cdot 10^8$ dyne/cm^2 (multilayers at a relative vapor pressure of 0.66). For 2:1 SOPC/C bilayers containing 4 mol% PEG-lipid, the lamellar repeat period ranged from 170.0 Å at $P = 4.0 \cdot 10^4$ dyne/cm^2 (liposomes in 3% PVP in 100 mM NaCl) to 105.7 Å at $P = 2.8 \cdot 10^7$ dyne/cm^2 (multilayers at a relative vapor pressure of 0.98). For the specimens containing the PEG-lipid, at higher applied pressure than $1.0 \cdot 10^8$ dyne/cm^2 (lower relative vapor pressures) additional low-angle reflections were observed with spacings corresponding to pure SOPC/C bilayers. This indicates that phase separation occurred at these higher applied pressures. In this paper we analyze only the data obtained for pressures $3.0 \cdot 10^3$ dyne/cm$^2 < P < 1.0 \cdot 10^8$ dyne/cm^2, where a single lamellar phase was present for all specimens examined.

All SOPC/C specimens contained 4 or 5 orders of diffraction, whereas the SOPC/C/PEG-lipid specimens usually contained only 3 or 4 orders. However, the SOPC/C/PEG-lipid specimen at the highest applied pressure ($P = 2.8 \cdot 10^7$ dyne/cm^2) contained 8 orders of diffraction, so that this diffraction pattern was at comparable resolution ($d/2h_{max} \approx 6$ Å) to all of the SOPC/C specimens. Structure factors for all of the SOPC/C data and the SOPC/C/PEG-lipid specimen at $P = 2.8 \cdot 10^7$ dyne/cm^2 are shown in Fig. 2. The solid line is the continuous Fourier transform for the

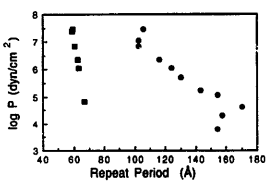

Fig. 1. Plot of logarithm of applied pressure (log P) versus lamellar repeat period for 2:1 SOPC/C bilayers in the absence (■) and presence of 4 mol% PEG-lipid (●). Osmotic stress experiments were performed on oriented multilayers in relative humidity atmospheres (log $P = 7.5$) and on unoriented liposomes in polymer solutions (log $P < 7.5$). For the liposome experiments, the stressing solutions contained 100 mM NaCl.

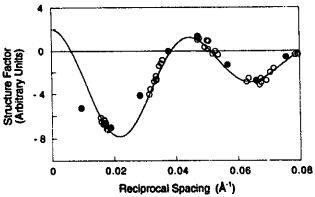

Fig. 2. X-ray structure factors for 2:1 SOPC/C bilayers in the absence (○) and presence (●) of 4 mol% PEG-lipid plotted versus reciprocal space coordinate. The solid line is the continuous transform for the SOPC/C data calculated using the sampling theorem as described in the text.

SOPC/C data calculated using the sampling theorem [52] and one particular data set. The phases for the SOPC/C data were calculated using the same analysis as detailed in McIntosh and Holloway [53] and are the same as those previously obtained from 2:1 egg PC/C bilayers [43]. Since all of the SOPC/C structure factors fall close to this line, the structure of this bilayer is approximately constant at all applied pressures [41,43,56]. For the SOPC/C/PEG-lipid specimen most of the structure factors fall close to this continuous transform, although, the structure factors corresponding to the first and third orders of diffraction fall slightly off the transform (Fig. 2).

Electron density profiles

Fig. 3 shows electron density profiles for both SOPC/C (top) and SOPC/C/PEG-lipid (bottom) at the same applied pressure of $2.8 \cdot 10^7$ dyne/cm^2. In this figure, two adjacent unit cells are shown. In the bilayer on the left side of each profile, the high density peaks, located at about ±25 Å from the bilayer center, correspond to the high density lipid headgroups and the lower electron density region in the center of the profile corresponds to the lipid hydrocarbon chains. 'Stick figure' representations of the lipids and PEG-lipids are included in the figure to identify these regions of the bilayer. The medium density region between head group peaks from adjacent bilayers corresponds to the fluid space between adjacent bilayers. Note that the fluid space is much wider for the bilayers containing the PEG-lipids.

Fig. 4 shows electron density profiles from the same SOPC/C and SOPC/C/PEG-lipid bilayers superimposed so that the organization of the bilayer interiors can be more readily compared. In this figure only one unit cell is shown. From −25 Å to +25 Å the two profiles superimpose quite closely. The distance between the headgroup peaks across the bilayer is quite similar for the bilayers with and without PEG-lipids.

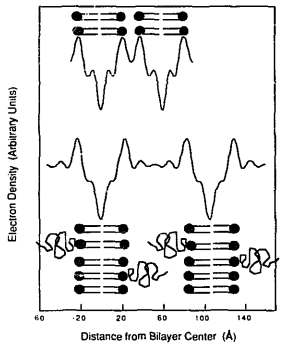

Fig. 3. Electron density profiles for 2:1 SOPC/C bilayers in the absence (top) and presence (bottom) of 4 mol% PEG-lipid. For each profile two unit cells are shown. Stick figure models are included to show the positions of the lipid molecules in the profiles. In these stick figures, the circles represent the phospholipid headgroups, the straight lines represent the hydrocarbon chains, and the curvy lines represent the attached PEG.

The peak-to-peak separation across the bilayer is 44.7 Å ± 0.8 Å (mean ± S.D. for nine osmotic stress experiments) for SOPC/C bilayers and 45.5 Å (one experiment at $P = 2.8 \cdot 10^7$ dyne/cm^2) for the SOPC/C/PEG-lipid bilayer.

These profiles can now be used to estimate the distance between the edges of the SOPC/C bilayers. As noted previously [41–43], the definition of the lipid/water interface is somewhat arbitrary, because the bilayer surface is not smooth, the lipid headgroups are mobile [57], and water penetrates into the headgroup region of the bilayer [58,59]. We operationally define the bilayer width as the total thickness of the

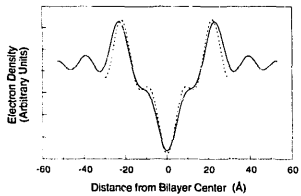

Fig. 4. Electron density profiles for 2:1 SOPC/C bilayers in the absence (dashed line) and presence (solid line) of 4 mol% PEG-lipid. One unit cell is shown for each profile.

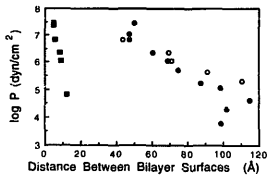

Fig. 5. Plot of logarithm of applied pressure (log P) versus the distance between the surfaces of adjacent bilayers composed of 2:1 SOPC/C in the absence (■) and presence of 4 mol% PEG-lipid (●) in 100 mM NaCl. Also shown are data for SOPC/C/PEG-lipid in 1 mM NaCl (○).

SOPC/C bilayer assuming that the phosphocholine headgroup conformation is the same as it is in single crystals of dimyristoylphosphatidylcholine [60]. That is, we assume that the phosphocholine group is, on average, oriented approximately parallel to the bilayer plane. Since at this resolution the high density headgroup peaks in the electron density profile are known to be located between the phosphate moiety and the glycerol backbone of the lipid [61,62], the 'physical' edge of the bilayer lies about 5 Å outward from the center of the high density peaks in the electron density profiles [41,42,47]. Thus, we estimate the total SOPC/C bilayer thickness to be the distance between headgroup peaks in the profiles plus 10 Å. With these assumptions, the distance between the surfaces of the SOPC/C bilayers can be calculated for each osmotic stress experiment by subtracting the total bilayer thickness (54.7 Å for SOPC/C and 55.5 Å for SOPC/C/PEG-lipid) from the lamellar repeat period.

Applied pressure versus interbilayer separation

Fig. 5 shows a plot of the logarithm of applied pressure versus the distance between the surfaces of adjacent SOPC/C bilayers in the presence and absence of 4 mol% PEG-lipid. For all applied pressures the presence of the PEG-lipid markedly increases the fluid space between bilayers. For example, at the lowest applied pressure the fluid separation is increased by about 100 Å.

Fig. 5 also compares osmotic stress data taken from liposomes in polymer solutions in 100 mM NaCl and 1 mM NaCl. For SOPC/C bilayers, the interbilayer separation is nearly the same in 100 mM and 1 mM NaCl (not shown), whereas for SOPC/C/PEG-lipid bilayers interbilayer separation is larger in 1 mM NaCl compared to 100 mM NaCl especially at lower applied pressures. For log $P < 5$, lamellar diffraction was not obtained for SOPC/C/PEG-lipid suspensions in 1 mM NaCl, indicating indefinite swelling of the multilayers.

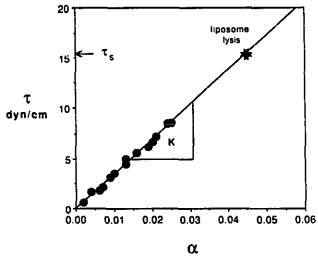

Fig. 6. Membrane stress versus membrane areal strain. Increasing the membrane tension caused a linear increase in liposome membrane area. The slope of this line $\Delta\tau/\Delta\alpha$, for membrane tensions greater than ~0.5 dyne/cm, is the elastic area expansion modulus K, which for this particular liposome was 345 dyne/cm. Subsequent increases in membrane tension produced failure of the membrane and lysis of the liposome at some critical areal strain α_c, and tensile strength τ_s.

Micropipet manipulation

Membrane isotropic tension was plotted versus membrane area change to give a direct measure of the elastic area expansion modulus K and and tensile strength τ_s for 2:1 SOPC/C bilayers containing 4 mol% PEG-lipid (Fig. 6). For single walled liposomes, the average area expansion modulus was obtained from the slope of these stress vs. strain plots to be 343 ± 67 dyne/cm and the average tensile strength was determined from the maximum stress at failure to be 16.5 ± 2.5 dyne/cm. These values are similar to those previously recorded for SOPC/C bilayers [32].

Using the dual micropipet method to make a direct test of the expected non-adherence property on individual Stealth liposomes, we observed that SOPC/C 2:1 liposomes with 4 mol% PEG-lipid did not show any tendency to spread on each other upon maneouvering into contact; they simply undulated freely when not supported by micropipet suction pressure. No measureable level of adhesion was detected.

Discussion

Structure of bilayers containing PEG-lipids

The electron density profiles (Figs. 3 and 4) demonstrate that the incorporation of 4 mol% PEG-lipid into SOPC/C does not appreciably modify the organization of the bilayer interior. The invariance of the structure and thickness of the bilayer hydrocarbon region upon the addition of PEG-lipid is consistent with our micromanipulation studies which showed that the elastic area expansion modulus and tensile strength are also unchanged by the incorporation of the same amount of PEG-lipid. Since it has previously been found that K depends strongly on the area per lipid molecule [32], the invariance of K with incorporation of PEG-lipid is consistent with the same bilayer thickness for SOPC/C in the presence and absence of PEG-lipid.

Origin of interbilayer repulsive pressure

For applied pressures ranging over five orders of magnitude, both the lamellar repeat period (Fig. 1) and distance between adjacent bilayer surface (Fig. 5) are considerably larger upon the incorporation of 4 mol% PEG-lipid. Thus, the pressure–distance relations (Fig. 5) showed that the incorporation of PEG-lipids increases both the magnitude and the range of the repulsive pressure between adjacent SOPC/C bilayers. Based on these data we now argue that this repulsive pressure must be mainly a steric pressure, and can not be primarily due to increases in the other repulsive pressures that have been shown to act between apposing bilayers, namely the hydration, electrostatic, and undulation pressures. We consider in turn each of these repulsive pressures.

The hydration pressure associated with bound water at the bilayer/water interface is always short-ranged [41,49]; it has never been observed to be larger than the van der Waals attractive pressure for distances greater than about 20 Å [40,41,49,63]. Therefore, the hydration repulsion cannot by itself account for the large (up to 100 Å) increase in observed fluid space caused by the PEG-lipid.

The PEG-lipid headgroup bears a negative charge and so it was also important to evaluate the relative contribution of electrostatic repulsion. This repulsive pressure can be estimated from our data taken as a function of NaCl concentration, since the magnitude of electrostatic pressure between two charged plates is proportional to the bulk salt concentration [64]. Although there is a slight difference in the pressure–distance profiles observed in 1 and 100 mM NaCl solutions, this difference is small for applied pressures greater than 10^5 dyne/cm, i.e., for bilayer separations less than 100 Å. This implies that the electrostatic contribution to the total pressure is also relatively small in these ranges of pressure and distance. In contrast, for applied pressures less than 10^5 dyne/cm, apposing bilayers swell up to a finite separation in 100 mM NaCl but swell apart indefinitely in 1 mM NaCl. This implies that at low ionic strengths electrostatic repulsion can in fact play a role in the nature of the interactions between bilayers at low applied pressures and large separations. However, since the ionic strength in plasma is ~300 mM, our data indicates that electrostatic repulsion does not contribute appreciably to the total repulsive pressure caused by PEG-lipids in blood circulation.

The contribution of undulation pressure, which depends on the curvature elastic properties of the bilayer, must also be quite small for several reasons. First, the undulation pressure for bilayers containing this amount of cholesterol is usually weak [65], due to the higher moduli for area expansion [32] and bilayer curvature [66]. Our micromanipulation experiments show that the incorporation of PEG-lipid does not change (lower) the area expansion modulus, and therefore cannot appreciably modify the undulation pressure. Moreover, similar pressure distance relations are observed for 4 mol% PEG-lipid in both liquid-crystalline (Fig. 5) and gel phase DSPC bilayers [67] demonstrating that the same repulsive pressures are given by rigid (non-undulating) bilayers. Thus, the major portion of the increased repulsive pressure in bilayers containing PEG-lipid at ionic strengths of 100 mM or greater must be caused by a steric pressure.

Polymer extension away from the bilayer surface

We expect that the non-adsorbing, but grafted PEG of this molecular weight (1900 g/mol) at this surface density, has an extension away from the surface of ~ 50 Å. This expectation is based on scaling theories [37–39] that also predict that a repulsive pressure should only develop when the two surface polymer layers begin to overlap. A measure of the extension of the polymer away from the surface can therefore be obtained from our osmotic pressure data (Fig. 5) which show that the repulsive pressure begins at an interbilayer gap of about 100 Å, in close agreement with twice the theoretical polymer extension of ~ 50 Å. We are currently in the process of collecting pressure-distance data as a function of both the molecular weight of the PEG moiety and the concentration of PEG-lipid in the bilayer so that we can provide direct tests of these theoretical treatments [39], including the magnitude of the repulsion [39,67].

Role of the repulsive barrier in blood circulation of Stealth liposomes

The main result from several studies of *in vivo* circulation times is that whilst free drug is rapidly cleared from the bloodstream in only a few minutes and 'conventional' liposomes are essentially cleared with a circulating half-life of ~ tens of minutes, the circulating half-life of liposomes modified with the PEG lipid is on the order of tens of hours. Thus, 24 h after intravenous injection, a relatively high percentage (~ 50%) of the injected dose can still be found in the bloodstream. A comparison between these data and the interbilayer separation data of Fig. 3 and Fig. 5 shows that the longer circulation times recorded for PEG liposomes correlates with an increase in the size of the interbilayer gap and range of repulsion. Thus, we can now argue that the increased circulation times are a direct consequence of the measured steric repulsive barrier properties of PEG lipid.

What this data implies is that the interaction of macromolecules such as plasma proteins and cellular surfaces with bilayers containing PEG-lipid is probably limited to a distance of ~ 50 Å from the phospholipid surface. This barrier would then likely inhibit the kinds of contact-destabilization that plasma lipoproteins appear to exert on the lipid molecules of unmodified lipid bilayers, the opsonization of the liposome, and the adhesive recognition by phagocytosing cells.

In the absence of surface polymer, neutral lipid bilayers (and bilayers with less than 5 mol% charge) will approach to within 10 Å–20 Å of each other before the repulsive hydration pressure opposes closer approach. At this small separation distance, the bilayers spread on each other, adhere and enter an attractive, free energy minimum because of the action of interbilayer van der Waals forces [23,27]. For PEG-lipid bilayers, it is expected that interbilayer attraction due to van der Waals forces will not come into play because of the much larger distances of separation. In our micropipet test, no measureable level of adhesion was observed, which indicates that mutual polymer repulsion can in fact overcome the van der Waals attraction between lipid bilayers [23,27]. We plan to use this experimental method to determine whether adhesion occurs between Stealth liposomes and a range of cellular surfaces by replacing the test liposome with a test cell. This direct test will allow us to more fully explore the role of RES recognition and binding on liposome uptake and removal from the circulation.

It is also important to mention that our measures of the polymer extension length are useful in the design of immuno-Stealth liposomes where a specific receptor moiety is incorporated along with the PEG-lipid [68]. In order for the receptor to be available for binding whilst the lipid surface is still protected, the distance that the receptor extends from the surface will likely have to be matched by the grafted polymer extension.

Finally, the measurements of lipid bilayer elasticity showed that the elastic area expansion modulus for the PEG-lipid containing bilayers was essentially the same as that measured previously for unmodified SOPC/C liposomes [32]. Thus, the mechanical stability of Stealth liposomes was unaltered by the incorporation of PEG-lipid, and was still dominated by the phospholipid and cholesterol components. From this we may infer that the increased *in vivo* circulation times for the Stealth formulation cannot be due to an enhanced mechanical cohesion, which indirectly supports our conclusions from X-ray that steric stabilization is the primary mechanism. These results also imply that high mechanical cohesion of the lipid bilayer may not be a prerequisite when access to the lipid surface is inhibited by PEG-lipid. This feature makes the Stealth liposome

a very versatile construct with regard to lipid composition when one now considers designing for the release of drug from the liposome interior at the delivery site.

Conclusions

Our data confirm the previous postulations that membrane-bound polymeric PEGs (1900 g/mol), can exert a significant interbilayer repulsion [5–12]. Moreover, they show for this particular PEG molecular weight and surface concentration that the polymer chain extends a distance of ~50 Å from the lipid bilayer surface. The repulsive properties of this polymeric barrier correlate with the longer *in vivo* circulation time that is observed for Stealth liposomes and this correlation provides direct support for the hypothesis that the origin of the Stealth property lies in a steric stabilization mechanism. Thus, these measurements strongly suggest that the molecular origin of PEG-liposome stability in blood circulation is a consequence of the extended conformation of PEG polymer at the surface which inhibits mutual aggregation and likely reduces interactions with plasma proteins and phagocytic cells that normally lead to conventional liposome disintegration and uptake. In addition, our micromechanical measurements on giant liposomes show that the increased circulation time for Stealth liposomes is not related to any augmentation of mechanical stability due to the incorporation of PEG-lipid.

Acknowledgements

This work was supported by grants GM 27278 and GM 40162 from the National Institutes of Health. We would also like to thank Liposome Technology Inc., for supplying the PEG-lipid. David Needham is grateful to the Alfred M. Hunt Fund for the Hunt Faculty Scholarship Award.

References

1 Illum, L. and Davis, S.S. (1987) Life Sci. 40, 1553–1560.
2 Gregoriadis, G. (1989) News Physiol. Sci. 4, 146–151.
3 Allen, T.M. and Chonn, A. (1987) FEBS Lett. 223, 42–46.
4 Hershfield, M.S. and Buckley, R.H. (1987) N. Engl. J. Med. 316, 589.
5 Klibanov, A.L., Maruyama, K., Torchilin, V.P. and Huang, L. (1990) FEBS Lett. 268, 235–237.
6 Blume, G. and Cevc, G. (1990) Biochim. Biophys. Acta 1029, 91–97.
7 Mayhew, E., Lasic, D., Babbar, S. and Martin, F.J. (1992) Int. J. Cancer 51, 1–8.
8 Papahadjopoulos, D., Allen, T., Gabizon, A., Mayhew, E., Matthay, K., Huang, S.-K., Lee, K., Woodle, M.C., Lasic, D.D., Redemann, C. and Martin, F.J. (1991) Proc. Natl. Acad. Sci. USA 88, 11460–11464.
9 Senior, J., Delgado, C., Fisher, D., Tilcock, C. and Gregoriadis, G. (1991) Biochim. Biophys. Acta 1062, 77–82.
10 Mori, A., Klibanov, A.L., Torchilin, V.P. and Huang, L. (1991) FEBS Lett. 284, 263–266.
11 Allen, T.M., Hansen, C., Martin, F., Redmann, C. and Yan-Yeung, A. (1991) Biochim. Biophys. Acta 1066, 29–36.
12 Allen, T.M., Austen, G.A., Chonn, A., Lin, L. and Lee, K.C. (1991) Biochim. Biophys. Acta. 1061, 56–64.
13 Allen, T.M. (1989) in UCLA Symposium on Molecular and Cellular Biology, Liposomes in the Therapy of Infectious Diseases and Cancer (Lopez-Bernstein, G. and Fidler, I., eds., Vol. 89, p. 405.
14 'Stealth' is a registered trademark of Liposome Technology Inc.
15 Lee, J.H., Kopecek, J. and Andrade, J.D. (1989) J. Biomed. Mater. Res. 23, 351–368.
16 Prime, K.L. and Whiteside, G.M. (1991) Science 252, 1164–1167.
17 Desai, N.P. and Hubble, J.A. (1991) J. Biomed. Mater. Res. 25, 829–843.
18 Jeon, S.I., Lee, J.H., Andrade, J.D. and DeGennes, P.G. (1991) J. Coll. Int. Sci. 142, 149–158.
19 Jeon, S.I. and Andrade, J.D. (1991) J. Colloid. Interface Sci. 142, 159–166.
20 Tirrell, M. (1991) Adv. Polymer Sci. 100, 31.
21 Yoshioka, H. (1991) Biomaterials 12, 861–864.
22 Lasic, D.D., Martin, F.J., Gabizon, A., Huang, S.K. and Papahadjopoulos, D. (1991) Biochim. Biophys. Acta 1070, 187–192.
23 Evans, E. and Needham, D. (1987) J. Phys. Chem. 91, 4219–4228.
24 Evans, E., Needham, D. and Jansen, J. (1987) in Proteins at Interfaces (Brash, J.L. and Horbett, T.A., eds.), pp. 88–103, American Chemical Society, Washington, DC
25 Evans, E. and Needham, D. (1988) in Molecular Mechanisms of Membrance Fusion (Ohki, S., Doyle, D., Flanagan, T.D., Hui, S.W. and Mayhew, E., eds.), pp. 83–99, Plenum Press, New York and London.
26 Evans, E. and Needham, D. (1988) Macromolecules 21, 1822–1831.
27 Needham, D. (1992) in Membrane Fusion Techniques (Düzgünes, N., ed.), Academic Press, in press.
28 Scherphof, G., Roerdink, F., Waite, M. and Parks, I. (1978) Biochim. Biophys. Acta 542, 296–307.
29 Chonn, A., Semple, S.C. and Cullis, P.R. (1991) Biochim. Biophys. Acta 1070, 215–222.
30 Chonn, A. and Cullis, P.R. (1992) in Journal of Liposome Research, Forum on Covalently Attached Polymers and Glycans to Alter the Biodistribution of Liposomes (Huang, L., ed.), in press.
31 Senior, J. (1987) Crit. Rev. Ther. Drug Carr. Syst. 3, 123–193.
32 Needham, D. and Nunn, R.S. (1990) Biophys. J. 58, 997–1009.
33 DeGennes, P.G. (1988) in Physical Basis Of Cell-Cell Adhesion (Bongrand, P., ed.), pp. 39–60, CRC Press, Boca Raton, FL.
34 Patel, S. and Tirrell, M. (1988) Colloids Surf. 31, 157–179.
35 Milner, S.T. (1991) Science 251, 905–914.
36 Arnold, K., Lvov, Y.M., Szogyi, M. and Gyorgyi, S. (1986) Stud. Biophys. 113, 7–14.
37 Alexander, S. (1977) J. Phys. (Paris) 38, 983.
38 DeGennes, P.G. (1980) Macromolecules 13, 1069.
39 Needham, D., Hristova, K., McIntosh, T.J., Dewhirst, M., Wu, N. and Lasic, D.D. (1992) in Journal of Liposome Research, Forum on Covalently Attached Polymers and Glycans to Alter the Biodistribution of Liposomes (Huang, L., ed.), in press.
40 LeNeveu, D.M., Rand, P.R., Parsegian, V.A. and Gingell, D. (1977) Biophys. J. 18, 209–230.
41 McIntosh, T.J. and Simon, S.A. (1986) Biochemistry 25, 4058–4066.
42 McIntosh, T.J., Magid, A.D. and Simon, S.A. (1987) Biochemistry 26, 7325–7332.
43 McIntosh, T.J., Magid, A.D. and Simon, S.A. (1989) Biochemistry 28, 7904–7912.
44 Simon, S.A. and McIntosh, T.J. (1989) Proc. Natl. Acad. Sci. USA 86, 9263–9267.
45 Parsegian, V.A. and Rand, R.P. (1989) Biochim. Biophys. Acta 988, 351–376.

46 McIntosh, T.J., Magid, A.D. and Simon, S.A. (1989) Biophys. J. 55, 897–904.
47 McIntosh, T.J., Magid, A.D. and Simon, S.A. (1990) Biophys. J. 57, 1187–1197.
48 Parsegian, V., Rand, R.P., Fuller, N. and Rau, D. (1986) Methods Enzymol. 127, 400.
49 Parsegian, V.A., Fuller, N. and Rand, R.P. (1979) Proc. Natl. Acad. Sci. USA 76, 2750–2754.
50 Blaurock, A.E. and Worthington, C.R. (1966) Biophys. J. 6, 305–312.
51 Herbette, L., Marquardt, J., Scarpa, A. and Blasie, J.K. (1977) Biophys. J. 20, 245–272.
52 Shannon, C.E. (1949) Proc. Inst. Radio Eng. N.Y. 37, 10–21.
53 McIntosh, T.J. and Holloway, P.W. (1987) Biochemistry 26, 1783–1788.
54 Kwok, R. and Evans, E. (1981) Biophys. J. 35, 637–652.
55 Tardieu, A., Luzzati, V. and Reman, F.C. (1973) J. Mol. Biol. 75, 711–733.
56 Torbett, J. and Wilkins, M.H.F. (1976) J. Mol. Biol. 62, 447–458.
57 Hauser, H., Pascher, I., Pearson, R.H. and Sundell, S. (1981) Biochim. Biophys. Acta 650, 21–51.
58 Worcester, D.L. and Franks, N.P. (1976) J. Mol. Biol. 100, 359–378.
59 Simon, S.A. and McIntosh, T.J. (1986) Methods Enzymol. 127, 511–521.
60 Pearson, R.H. and Pascher, I. (1979) Nature (Lond.) 281, 499–501.
61 Lesslauer, W., Cain, J.E. and Blasie, J.K. (1972) Proc. Natl. Acad. Sci. USA 69, 1499–1503.
62 Hitchcock, P.B., Mason, R., Thomas, K.M. and Shipley, G.G. (1974) Proc. Natl. Acad. Sci USA 71, 3036–3040.
63 McIntosh, T.J., Simon, S.A., Needham, D. and Huang, C.-h (1992) Biochemistry 31, 2020–2024.
64 Israelachvili, J.N. (1985) Intermolecular and Surface Forces with Applications to Colloidal and Biological Systems, Academic Press, London.
65 McIntosh, T.J., Magid, A.D. and Simon, S.A. (1989) Biochemistry 28, 17–25.
66 Evans, E. and Rawicz, W. (1990) Phys. Rev. Lett. 64, 2094–2097.
67 Needham, D., McIntosh, T.J. and Simon, S.A. (1992) Biophys. J. 61, A237.
68 Agrawal, A.K. and Allen, T.M. (1992) Biophys. J. 61, A493.